Efficient High Fidelity Signal Reconstruction Based on Level Crossing Sampling

Negar Riazifar, Nigel G. Stocks

Abstract—This paper proposes strategies in level crossing (LC) sampling and reconstruction that provide high fidelity signal reconstruction for speech signals; these strategies circumvent the problem of exponentially increasing number of samples as the bit-depth is increased and hence are highly efficient. Specifically, the results indicate that the distribution of the intervals between samples is one of the key factors in the quality of signal reconstruction; including samples with short intervals does not improve the accuracy of the signal reconstruction, whilst samples with large intervals lead to numerical instability. The proposed sampling method, termed reduced conventional level crossing (RCLC) sampling, exploits redundancy between samples to improve the efficiency of the sampling without compromising performance. A reconstruction technique is also proposed that enhances the numerical stability through linear interpolation of samples separated by large intervals. Interpolation is demonstrated to improve the accuracy of the signal reconstruction in addition to the numerical stability. We further demonstrate that the RCLC and interpolation methods can give useful levels of signal recovery even if the average sampling rate is less than the Nyquist rate.

Keywords—Level crossing sampling, numerical stability, speech processing, trigonometric polynomial.

I. Introduction

REAL-WORLD signals such as speech, ECG, EEG, neural activity, pressure, temperature and vibration sensors may vary rapidly for brief moments and then remain constant for some time [1]. These signals are non-stationary and temporally sparse. Synchronous signal processing architectures do not take into account the temporal sparsity of these signals and, hence, classical uniform sampling in time can result in a large number of samples that convey little or no information.

The inefficiency inherent in uniform sampling has led to an upsurge in interest in the design of asynchronous [2] analogue to digital converters (ADCs) that utilise event based sampling. In particular there is a considerable interest in level crossing (LC) ADCs [3], [4] due to their applications in embedded sensing systems. LC ADCs have been shown to have significant benefits over conventional ADCs, not least they offer the potential of a significant reduction in operating power when signals are temporally sparse [5]. The rapid proliferation of battery powered wearable technologies is further fuelling interest in these emergent technologies.

Of particular relevance to the work presented here is the use of LC ADCs to process audio signals. Hearing aids (HAs) were one of the original wearable devices and battery life is a critical design factor. High fidelity audio processing requires a relatively high effective number of bits (ENOBs). HAs digitize audio and speech signals with 20-24 bit precision to capture the large dynamic range and yield acceptable signal-to-noise ratio (SNR) at lower signal levels [6].

To date few studies have investigated the use of LC ADCs in the context of high-fidelity signal processing. Although the design of LC ADCs is well advanced the majority of studies report SNR or signal-to-noise-and-distortion-ratio (SNDR) of less than 60 dB [7]. Exceptions are reported by Kozmin [8] who achieved SNDRs in excess of 80 dB. However, the signals employed were pure-tone ultrasound signals that lacked the fine structure of speech and music. Wang [9] employed triangular dither to achieve similar performance; however the use of dither increases the sampling rate and hence negates the power saving achieved by LC ADCs.

Design principles have been established that can be applied to the development of high-resolution LC ADCs. The ENOBs is governed by the accuracy of the sampling process. Formula relating time and amplitude uncertainty to the SNR (and hence ENOBs [10]) give clear design targets. Whilst these formulae provide target criteria for the front-end analogue-to-digital conversion, no such design criteria are available for conversion back to the analogue domain. In practice digital-to-analogue conversion results in a signal reconstruction error that also needs to be considered. This is particularly the case when sampling is non-uniform in time because reconstruction methods are less well developed.

Reconstructing signal from non-uniform samples is an important issue in the area of DSP [11], [12]. Based on the generalised Nyquist criterion, a band-limited signal with bandwidth BW can be reconstructed from its non-uniform samples, if the average sampling rate is larger than $2BW$ [13]–[15]. There are different approaches of reconstruction from non-uniform sampling [13], [14], [16], including iterative approximation techniques [17], [18], frequency domain techniques [19], polynomial or spline interpolation [9], [20]–[23] and sinc-based reconstruction method [13]. Although these reconstruction methods have been applied to LC ADCs the fidelity of the reconstruction is relatively modest [24]. Furthermore, many of the reconstruction methods are numerically unstable due to ill-conditioning and hence unreliable [25].

Here we investigate reconstruction based on trigonometric polynomials and an adaptive weights least square approach [11]. Adaptive weights improve ill-conditioning and hence numerical stability and exact reconstruction has been proven for band-limited signals [11]; therefore this approach is a strong candidate for use in high fidelity systems.

N. Riazifar and N. G. Stocks are with the Department of Engineering, University of Warwick, Coventry, UK (e-mail: n.riazifar@warwick.ac.uk, n.g.stocks@warwick.ac.uk).

We also propose a sampling method that potentially reduces power consumption by reducing the sampling rate compared to conventional LC ADCs. The sampling method exploits our finding that significant redundancy can occur between LC generated samples. This sampling method could be modified for use in an asynchronous ADC, targeted for use in energy constrained applications.

This paper is organised as follows. After an introduction on the LC sampling approach in Section II, the reconstruction methodology is presented in Section III. Section IV outlines the accuracy of LC ADCs. In Section V we provide the proposed sampling and reconstruction methodologies. The simulation and results for speech signals are discussed in Sections VI and VII. Lastly, Section VIII concludes the paper.

II. Level Crossing Sampling

LC events, which are deemed to occur when the signal crosses a predefined threshold value provide non equi-spaced samples in time [26]. This sampling technique is called conventional LC (CLC). It is also known as sent-on-delta or implicit sampling [27]. The principle of CLC sampling is presented in Fig. 1. Reference amplitude thresholds are regularly distributed along the amplitude range of the signal. A sample is triggered when the input signal crosses one of these thresholds. Samples are non-uniformly distributed in time and are dependent on the statistics of the signal.

In the CLC sampling, the times $t_1, t_2, \cdots$ are considered instants at which the levels $q_a, q_b, \cdots$ are crossed (Fig. 1) [15]. For a signal $f(t)$ this yields the sample pairs $\{t_j, f_j\}$, $f(t_j) = f_j$. The samples can then be processed by an asynchronous DSP or interpolated to obtain uniform-in-time samples. Sampling times t_j depends only on the form of $f(t)$ and the threshold locations. This results in variable sampling rate; dense sampling occurs when the signal varies rapidly and less dense when the signal is slowly varying. The relationship between the bit-depth, B, and the number of thresholds, N, is usually defined as $N = 2^B$.

A review of methods in literature for LC sampling scheme is provided in [24], [28]–[30]. The potential benefits of asynchronous LC schemes are many folds. Power dissipation typically scales linearly with input activity [31] and hence will be reduced for signals that are temporally sparse [5].

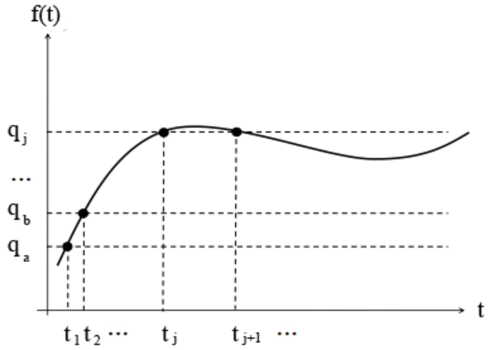

Fig. 1 Level crossing sampling, adapted from [15]

Consequently, LC ADCs are expected to consume lower power compared to their synchronous counterparts. LC technique saves not only dynamic power in both ADC and DSP but also bandwidth resources; because of the lower net sampling rate. Alias free sampling is another benefit of LC sampling [3].

III. Reconstruction from Irregular Samples

We consider the problem of reconstructing a band-limited function $f(t)$ from its set of irregular samples $\{f(t_j), j \in \mathbb{Z}\}$. An efficient, accurate and numerically stable reconstruction of $f(t)$ can, theoretically, be achieved by interpolating the data $f(t_j)$ using trigonometric polynomials of degree M [11], [25].

We used adaptive-weight conjugate-gradient Toeplitz reconstruction method (ACT algorithm) [25]. However, because we are implementing off-line analysis the inversion of the Toeplitz matrix is undertaken using standard least squares methods [11].

Kozmin [8] employed ACT reconstruction method in LC ADC. Our aim is to maximise the reconstruction accuracy based on this method. We apply ACT algorithm to the oversampling problem; we oversample the signal by increasing the bit-depth to get better resolution/accuracy while negating the negative impact of the exponentially increasing the number of sample points.

For any integer $M > 0$, the class of trigonometric polynomials is as follows,

$$P_M = \{p : p(t) = \sum_{k=-M}^{M} a_M(k) \frac{e^{\frac{2\pi ikt}{2M+1}}}{\sqrt{2M+1}}, a_M(k) \in \mathbb{C} \quad (1)$$

A unique trigonometric polynomial $p_M \in P_M$ of suitable degree and period fits the samples $f(t_j)$ in an interval $[-M, M]$. As the length $2M$ increases, p_M converges to the original function f. For the purpose of a local approximation of f, p_M is considered to have period $2M+1$ and order M. An upper bound for the degree of p_M is known as a consequence of band-limitedness [25]. In order to avoid the boundary effects, the samples are taken in $J_M \subseteq [-M-1, M+1]$ in which two adjacent samples are additionally taken.

A. Theorem

Suppose $\{t_j, f(t_j)\}, j \in \mathbb{Z}$ and $-M - \frac{1}{2} \leq t_1 < \cdots t_j < M + \frac{1}{2}$, is given and the sampling set satisfies the maximal gap condition (MGC) [25],

$$\sup(t_{j+1} - t_j) = \delta < \frac{1}{2f_{max}} = \frac{T_0}{2M}, j \in \mathbb{Z} \quad (2)$$

where δ is the largest interval in the whole sequence, T_0 is the record length, f_{max} is the maximum frequency in the trigonometric polynomial. Ideally, $p_M(t_j) = f(t_j)$. However, for finite M this is not equal, and the error should be minimized. The unique trigonometric polynomial, $p_M \in P_M$, solves least squares problem (LSP).

$$\sum_{j \in J_M} |p_M(t_j) - f(t_j)|^2 \frac{t_{j+1} - t_{j-1}}{2} = minimum \quad (3)$$

where the minimum is taken over all $p \in P_M$, then for all derivatives $l \geq 0$,

$$\lim_{M\to\infty} \int_{-M-1/2}^{M+1/2} |\, f^{(l)}(t) - p_M^{(l)}(t)\,|^2 \, dt = 0 \qquad (4)$$

and also $\lim_{M\to\infty} p_M(t) = f(t)$.

LSP is an accurate reconstruction method for irregular sampling problem which can be solved by the inversion of a Toeplitz matrix [11], [32]. C_M is considered the $(2M+1) \times (2M+1)$ positive Toeplitz matrix.

$$(C_M)_{kl} = \sum_{j\in J_M} \frac{w_j}{2M+1} e^{\frac{-2\pi i(k-l)t_j}{2M+1}}, |k|, |l| \leq M \qquad (5)$$

where $w_j = \frac{t_{j+1}-t_{j-1}}{2} > 0, j \in \mathbb{Z}$, is a set of weights and only changes the amplitude of the components. They help to keep the condition number of a Toeplitz matrix low [25].

B. Reconstruction Algorithm

Suppose the sequence of LC samples $\{(t_j, f(t_j)), j \in J_M\}$ is given as an input, $w_j > 0, j \in \mathbb{Z}$ and condition $J_M \geq 2M+1$ is satisfied. $b_M \in \mathbb{C}^{2M+1}$ is computed as follows [11],

$$b_M(k) = \sum_{j\in J_M} f(t_j) \frac{w_j}{\sqrt{2M+1}} e^{\frac{-2\pi ikt_j}{2M+1}}, |k| \leq M \qquad (6)$$

We can construct the trigonometric polynomial using (1). a_M is the matrix of the Fourier coefficient and can be calculated by the inversion of C_M.

$$a_M = C_M^{-1} b_M \in \mathbb{C}^{2M+1} \qquad (7)$$

Then for all $p \in P_M, p \neq p_M$,

$$\sum_{j\in J_M} |p_M(t_j) - f(t_j)|^2 w_j < \sum_{j\in J_M} |p(t_j) - f(t_j)|^2 w_j \qquad (8)$$

We expect this trigonometric polynomial to give good reconstruction results. Feichtinger [25] proved that oversampling improves the condition number of the reconstruction problem. Oversampling is not a problem in this algorithm. Because the number of frequency components M dictates the size of the Toeplitz matrix, not the number of data points.

ACT algorithm uses a weighted LS method and this weighting improves the condition number of the Toeplitz matrix; therefore it gives rise to improve the numerical stability and therefore should give rise to better quality of reconstruction.

MGC is the limiting factor of the application of this method; if the gap size between samples is too large, there is no guarantee that the trigonometric polynomial converges to the signal we are trying to reconstruct [11]. This theory therefore only applies to LC ADCs if the bit-depth is high enough. This is a fundamental limitation on the reconstruction of the irregular samples.

IV. Accuracy

It is well established that the accuracy of a LC ADC is governed by a number of factors that in practice are hardware dependent; specifically, errors occur in the LC sample pairs $\{t_j, f_j\}$. The sample level f_j equals the value (voltage) of the threshold that was crossed when the jth sample was generated. In practice, the threshold levels are only known to finite precision. Errors also occur in the specification of the sampling instants. Continuous time LC ADCs introduce unwanted jitter in the instants t_j due to the finite response time of the electronic comparators and internal noise. For discrete-time ADCs time t_j is mapped onto the nearest clock interval and hence quantization noise is introduced.

For the purpose of this study sampling errors are negated by specifying the samples to machine precision. Under these conditions the dominant source of error arises from the signal reconstruction [33]. This approach, therefore, enables the efficacy of the novel reconstruction and sampling methods to be evaluated directly without contamination from other sources of error.

It is common practice to quantify different sources of errors independently, enabling the dominant sources to be identified. For example, the fundamental performance of standard uniform sampled ADCs is often cited in terms of the SNR as,

$$SNR_{dB} = 6.02B + 1.76 \qquad (9)$$

This quantifies the noise arising from quantising the sample levels with bit-depth B when the signal is a full-scale sinusoidal signal. In practice other forms of noise and distortion further reduce the SNR and hence (9) is viewed as an upper limit on performance. More generally (9) is used to quantify the ENOBs from a known measure of the SNR [10],

$$ENOB = \frac{SNR_{dB} - 1.76}{6.02} \qquad (10)$$

V. Sampling and Reconstruction Methodologies

In principle oversampling can be realised in LC ADCs through increasing the bit-depth B. Every additional bit doubles the number of thresholds and hence approximately doubles the number of samples; hence the number of samples is expected to depend exponentially on bit-depth.

The potential advantage of oversampling is not only an increase in the ENOB but also enhanced numerical stability. A significant advantage of employing an adaptive-weights Toeplitz formalism is that the numerical conditioning is theoretical well established [25]. The condition number of the Toeplitz matrix has been rigorously obtained,

$$cond\, C_M \leq \left(\frac{1+2\delta M}{1-2\delta M}\right)^2 \qquad (11)$$

It is notable that the conditioning of the problem is governed entirely by the maximal gap δ and the order of the polynomial M. Reducing δ (e.g. by increasing B) clearly improves the condition number and may be expected therefore to enhance the accuracy of the reconstruction. In CLC sampling large gaps between samples can occur naturally and the MGC may be violated. Such a situation is expected to lead to numerical instability. However, an obvious disadvantage of increasing bit-depth is that fast moving portions of the signal will be over represented and the number of samples will increase exponentially with B. Potentially this will negate the benefit of the reduced power consumption of an LC ADC.

Our proposed sampling algorithm aims to achieve the benefits of oversampling by increasing bit-depth but to avoid the exponential increase in the number of samples. Two approaches are investigated and combined, one that exploits redundancy in the parts of the signal that are over represented and another that interpolated samples to reduce δ.

First, we introduce what we term the reduced CLC (RCLC) algorithm.

The first step is to perform CLC sampling as explained in Section 2. This gives a set of sample pairs $\{t'_j, f'_j\}$. For high bit-depth the set $\{t'_j, f'_j\}$ is large and reconstruction is computationally expensive. We therefore remove samples that are 'close together'. Sample t'_{j+1} is removed if $\Delta'_j < T_{min} = C * T_N = C * \frac{1}{2BW}$, $\forall \Delta'_j$, where $\Delta'_j = t'_{j+1} - t'_j$, T_{min} is the minimum temporal difference between samples, T_N is the inverse of the Nyquist frequency, BW is the bandwidth of the original signal and $C > 0$ is a coefficient that enables control over T_{min}. This procedure leads to a reduced LC sample set with new sample pairs $\{t''_j, f''_j\}$ with a new time interval $\Delta''_j = t''_{j+1} - t''_j$.

Removing samples is designed to reduce redundancy between samples but the MGC might not be satisfied for some samples. An additional interpolations step is therefore introduced. New samples are inserted if $\Delta''_j > T_{max} = \frac{T_0}{2M}$, where we introduce T_{max} as the maximum temporal difference between samples. First order interpolation between adjacent samples $\{t''_j, f''_j\}$ and $\{t''_{j+1}, f''_{j+1}\}$ is employed to get the final LC pairs $\{t_j, f_j\}$ used to reconstruct the original signal. We term this algorithm RCLC sampling with interpolation or RCLCI.

Fig. 2 illustrates the four set of samples. It shows the variation between different sampling methods.

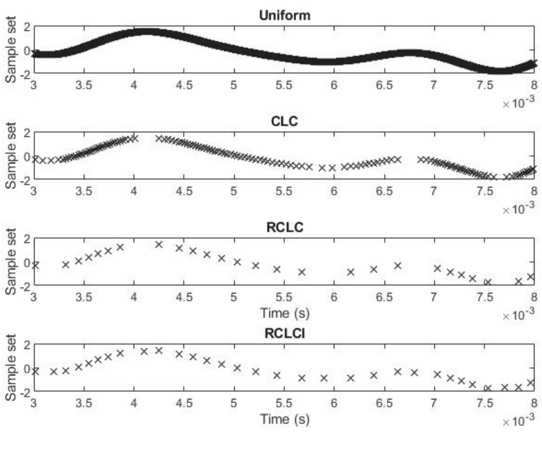

Fig. 2 An illustration of uniform, CLC, RCLC and RCLCI set of samples

In the RCLCI sampling algorithm, we are increasing the sampling rate where it is required in sparse periods and reducing the sampling rate where it is populated with data points. Applying this criterion provides minimum data samples which extracts the main features of the signal and presents more efficient distribution of non-uniform samples. Another main benefit of RCLCI sampling method is that we can save the RCLC instead of RCLCI data set since we can do the interpolation as a part of digital to analogue converter; This makes the proposed sampling method very efficient.

VI. Simulation

Simulations were carried out in MATLAB using a speech signal sourced from the TIMIT database [34]. Numerical simulation of LC sampling is non-trivial due to the discrete representation of samples stored on a computer. It was our intention to eliminate time quantization errors associated with the sampling process. It was, therefore, necessary to up-sample the original signal uniformly in time with a very high sampling rate, r_u, before extracting LC samples by thresholding.

Up-sampling gives rise to uniform samples $f[n] = f(t = nT)$, $n = 0, 1, 2, \cdots$ where T is the new sampling period. In practice the speech signals, originally acquired with a sampling frequency of 16kHz, were up-sampled to 100MHz to achieve a high r_u and enable highly accurate approximation of the LC samples. However, it does not affect the cost because in practice the algorithms are designed for continuous time signals and hence no up-sampling is required. The signal is up-sampled to approximate continuous time signals. In the limit $r_u \longrightarrow \infty$ the LC samples and those derived from the thresholding of uniform samples converge. However, to eliminate time quantisation each LC is replaced by its closest uniform sample. For example, if a threshold crossing occurs between samples $f[n]$ and $f[n+1]$ then the LC sample is identified as $f[n]$. This yields samples that are known to machine precision. This reduces the set of uniform sample pairs $\{t_n, f_n\}$ to a new set $\{t'_j, f'_j\}$ that represents a highly accurate approximation to the actual LC samples.

In practice the signal has to be processed in frames [7]. The up-sampled signal was partitioned into 50% overlapping frames, W_k each of duration T_0. W_k is called capture frame. We designate the central sub-frame within W_k as a separate frame, $w_k \subset W_k$, and call it the evaluation frame. w_k is of length $\frac{T_0}{2}$. The partitioning of these frames is illustrated in Fig. 3.

Preliminary investigations revealed that the reconstructed signal contained significant error at the ends of the frame.

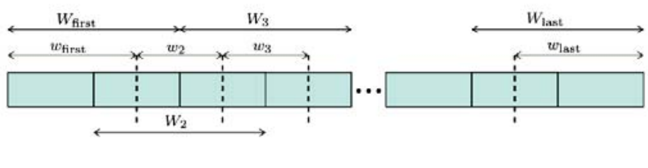

Fig. 3 Partitioning of signal into capture frames W_k and evaluation frames w_k, adapted from [7]

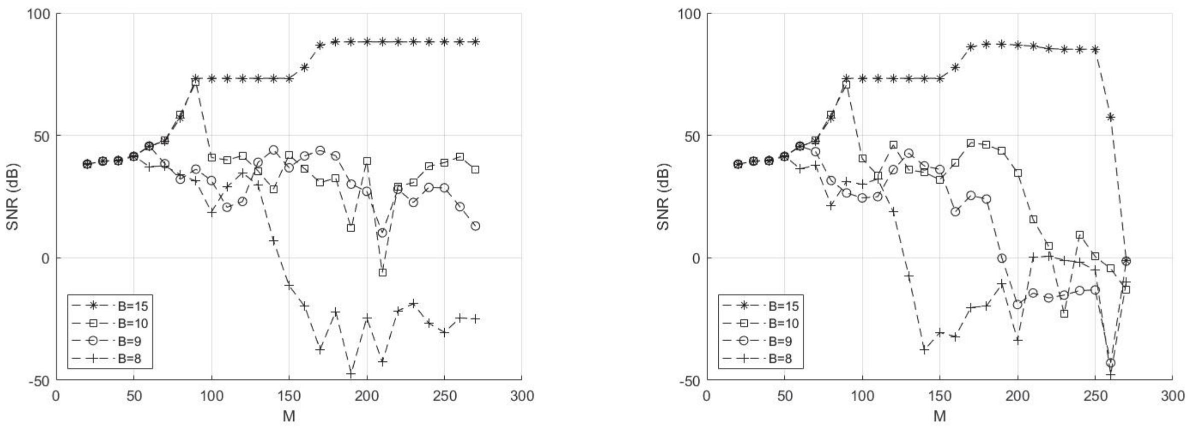

(a) (b)

Fig. 4 SNR Vs M using (a) CLC and (b) RCLC sampling methods on a windowed time speech frame for $C = 0.3$ and 8, 9, 10, 15 bit-depth

The error arose due to spectral leakage observed in the Fourier amplitudes a_M. Such effects were not considered in the original theoretical works [11] because convergence between the reconstructed signal and the original signal was proven in the limit $T_0 \longrightarrow \infty$ and hence windowing effects were eliminated. The use of a window function was observed to improve the results significantly. All results presented were for the Hanning window unless otherwise stated. The reconstructed signal was multiplied by the inverse window function before the accuracy of the reconstruction was assessed.

The thresholds were placed uniformly across the amplitude range of the signal. The peak-to-peak of the windowed frame was divided into 2^B intervals and the thresholds place at the midpoints of the intervals.

To further reduce end effects $\frac{1}{4}$ of each capture frame is discarded and only the reconstructed evaluation frames are saved. This method is similar to the overlap-add method [35]. The evaluation frames are then concatenated to reconstruct the whole signal. In all results presented we set $T_0 = 10$ms.

Accuracy of signal reconstruction is expressed using SNR between the original signal $f(t)$ and the reconstruction $p_M(t)$,

$$SNR = 10 \log \frac{\sum_n f^2[n]}{\sum_n \left(f[n] - p_M[n]\right)^2} \tag{12}$$

where $p_M[n] = p_M(t = nT)$.

VII. Results

A. Sample Redundancy and RCLC Sampling

The primary aim of the RCLC algorithm is to improve the energy efficiency of the sampling process by reducing the number of samples acquired. Whilst it may seem intuitive that samples closely spaced in time relative to the inverse bandwidth of the signal will contain redundant information, this problem has not been investigated in the context of LC ADCs. We, therefore, consider this question in this section.

Figs. 4(a) and (b) show SNR Vs M using CLC and RCLC samples. Clearly the SNR is strongly affected by the choice of M. The general dependence on M is the same for both CLC and RCLC sample sets. As M increases the fitted polynomial is able to capture more signal features (higher frequency content) and hence the SNR initially improves; but for sufficiently large M the MGC (2) becomes violated and numerical instability occurs. This results in unreliable reconstruction particularly at low bit-depth where the maximum gap δ is larger. Transition to unstable reconstruction is observed approximately at values of $M = 50, 60, 90$ for bit-depths of $8, 9, 10$ bits respectively.

Comparison between panels (a) and (b) clearly demonstrates that CLC samples are highly redundant; the same SNR is observed in both cases despite the removal of samples by the RCLC sampling scheme. Indeed, the degree of redundancy is remarkable. Table I shows the number of samples. For $B = 15$ the RCLC algorithm removes more than 99% of the samples and yet the maximal SNR is unchanged.

This observation has some interesting implications for sampling theory and in particular the design of LC ADCs. In conventional ADCs, increasing the sampling rate results in oversampling which in general leads to a higher ENOBs. Indeed one expects the SNR to improve as $20\log(OSR)$ where OSR is the oversampling ratio [36]. The results presented here demonstrate no improvement despite a significant increase in the average sampling rate. One is therefore led to conclude that the distribution of the time intervals of the samples has a strong bearing on performance. We speculate that the distribution is just as important as its mean value. Indeed, when interpreted with (11), our results suggest the SNR is predominantly impacted by a small number of larger intervals

TABLE I
Comparison of the Number of Samples Using CLC and RCLC Sampling Methods on a Windowed Time Speech Frame for $C = 0.3$

	$B = 8$	$B = 9$	$B = 10$	$B = 15$
CLC	1306	2610	5224	167004
RCLC	323	379	421	522

i.e. the tail of the distribution. This is consistent with the known instabilities that are observed if the MGC is violated.

Another interesting observation is that the SNR does not depend directly on the bit-depth i.e. increasing bit-depth does not necessarily lead to an increase in the SNR. In regions of stable reconstruction, the SNR is the same for all bit-depths and only depends on the value of M used in the reconstruction. However, increasing bit-depth reduces the maximum gap size δ thus enabling stable reconstruction at higher values of M. This observation leads to a practical recommendation for the choice of M. The maximum SNR is obtained at the largest value of M for which stable reconstruction can be achieved. This requires M to be selected such that the MGC is satisfied, this is achieved if $M = \frac{T_0}{2\delta}$. In practice slightly larger values of M may still lead to stable reconstruction and hence a higher SNR but this is not guaranteed.

We also note that ACT reconstruction method is capable of achieving SNRs close to 90 dB for $B = 15$. Indeed, preliminary numerical studies indicate that there is no upper limit to the achievable SNR if the bit-depth is chosen accordingly. Furthermore, Table I illustrates that the RCLC algorithm is capable of achieving high SNRs through the addition of a remarkably small number of samples. For example, increasing the bit-depth from $B = 10$ to $B = 15$ only adds approximately 25% more samples but enables an increase in SNR of more than 10 dB to be achieved. A similar improvement is observed for the original CLC samples but requires the processing of samples that are more than two orders of magnitude greater in number compared to RCLC.

Fig. 5 compares the number of RCLC samples to CLC samples as a function of bit-depth. The dashed line shows the number of samples that are required to satisfy the Nyquist criteria under conditions of uniform sampling. The input bandwidth of the signal is 8kHz and hence a sampling rate of 16KHz leads to 160 samples in a 10ms time window. As expected the number of CLC samples displays an exponential dependence on B. The effectiveness of the RCLC algorithm in reducing the number of samples is clear, particularly at larger bit-depth. Indeed, the proportion of new samples being added reduces with increasing B i.e. the dependence is sublinear as can be observed in the inset. This suggests the RCLC algorithm is computationally very efficient and can be combined with high bit-depth scenarios to realise any specified SNR.

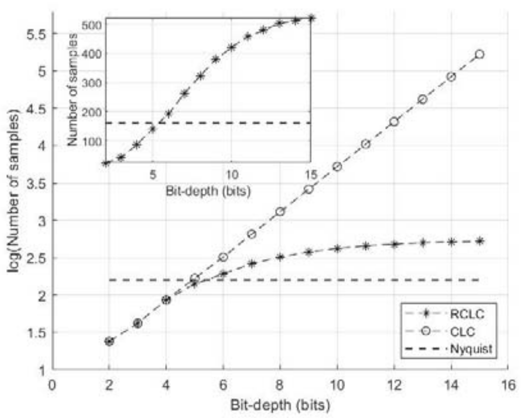

Fig. 5 Number of samples Vs bit-depth for $C = 0.3$ using RCLC and CLC methods for $M = 180$ and uniform sampling method for $M = 80$ on a windowed time speech frame

Fig. 6 shows the SNR and number of samples as a function of C for the RCLC data. C is a scaling factor that determines T_{min} and hence controls which CLC samples are rejected. If $C < 1$ samples are rejected that have intervals smaller than the minimum sampling period required to satisfy Nyquist criteria. $C = 1$ corresponds, approximately, to a RCLC sampling rate that just satisfies Nyquist criteria. $C > 1$ corresponds to undersampling.

It can be observed from Fig. 6 that C controls the redundancy between samples. The SNR is shown for two different values of M, $M = 50$, panel (b) and $M = 100$, panel (c). For both values of M the SNR plateaus for all bit-depths as C is reduced. No further increase in SNR occurs even though the number of samples continues to grow as C is decreased (panel (a)). There exists a critical value of C at which the SNR plateaus that is dependent on M and on the bit-depth, but in all cases inclusion of additional samples by reducing C beyond its critical value leads to no further useful information for signal reconstruction. These results demonstrate that the maximum SNR is dependent on C and M and choosing $C < 1$ does not guarantee the maximal SNR is obtained or that the minimum number of samples required to achieve the maximum SNR is realised. For example, for $M = 50$ the maximum SNR (at this value of M) can be attained for values of $C > 1$; indeed for $B = 15$ $C = 1.5$ yields the maximum SNR even though, notionally, the signal is now significantly undersampled. The number of samples for $B = 15$, $C = 1.5$ is approximately 100, which is less than the number of Nyquist samples 160. This efficient reconstruction occurs because at this value of M the bandwidth of the fitted polynomial is effectively less than the bandwidth of the original signal and hence regularisation leads to robust reconstruction. Only if C is so large that the MGC is violated does the SNR decrease.

A higher SNR can generally be obtained if M is increased but it is important to ensure the MGC is not violated. Fig. 6 (c) illustrates this point. For $B = 15$ the SNR is increased significantly compared to those for $M = 50$ but values of $C < 1$ are required to ensure the MGC is not violated. Indeed, for smaller bit-depth numerical instability is still impacting the SNR even at very small values of C because the MGC is violated in the original CLC samples.

B. RCLCI Sampling

The results of the previous section show that increasing M improves the SNR but ultimately numerical instability limits the maximum value of M that can be used. The instability occurs because the MGC is violated, specifically when $\delta > \frac{T_0}{2M}$, effects similar to the Runge effect [37] occur (Fig. 7). This significantly affects the signal reconstruction quality. Fig. 7 illustrates this point, high frequency oscillations are observed where adjacent samples violate the MGC. The amplitude of these oscillations increases as the gap size increases.

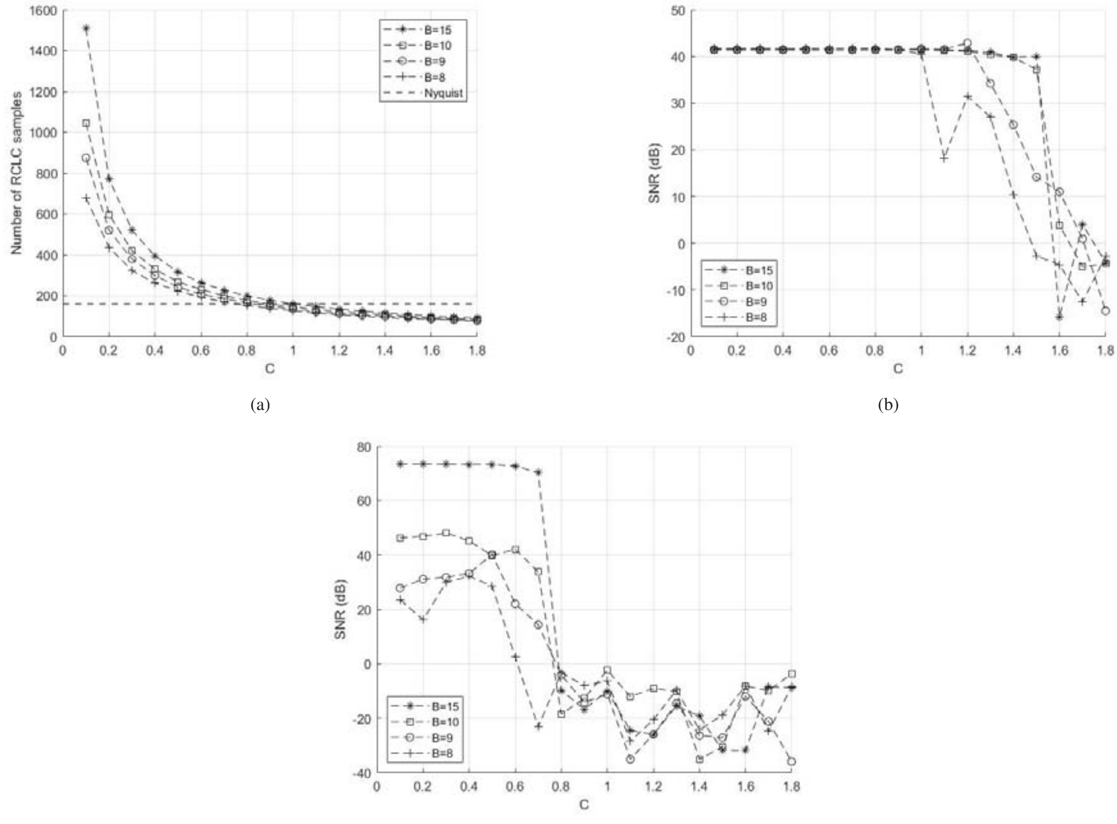

Fig. 6 (a) Number of RCLC samples and SNR of the RCLC samples Vs coefficient C for (b) $M = 50$ and (c) $M = 100$, on a windowed time speech frame for 8, 9, 10, 15 bit-depth

In principle, numerical instability can be reduced by using a high bit-depth to decrease δ but this approach cannot guarantee success because the value of δ depends on the statistics of the signal as well as the bit-depth. Therefore, in this section we use linear interpolation in conjunction with the RCLC sampling method. Interpolation adds additional samples between adjacent samples that violate the MGC. We call this the RCLCI algorithm. It is important to stress that interpolation is only introduced at the point of reconstruction and hence does not impact on the number of RCLC samples that would need to be stored or transmitted to achieve the SNRs reported here.

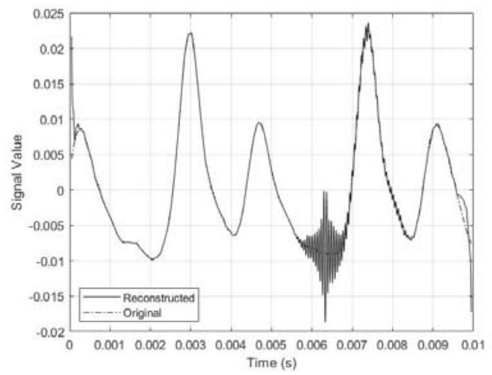

Fig. 7 Comparison of the original (dash-dotted line) and reconstructed (solid line) speech signals using RCLCI sampling method for $C = 0.3$, $M = 180$ and 10 bit-depth when MGC is not satisfied ($\delta > \frac{T_0}{2M}$)

In principle, LC sampling does not introduce quantisation error because, theoretically, the time-amplitude samples $\{t_j, f_j\}$ are known exactly in continuous time systems. However, sample points added using linear interpolation will introduce additional error because the exact value of the signal is unknown at the location of the inserted sample. We will see that this error introduces a form of a quantisation error.

Fig. 8 (a) shows SNR Vs M for RCLCI data points. The impact of the interpolation can be assessed by comparing with Fig. 4 (a). Three differences can be observed; first, higher SNRs can be achieved with lower bit-depths; second, and as expected, the erratic variation in SNR due to numerical instability is no longer observed and third, interpolation causes a saturation (plateauing) of the SNR at high values of M.

To understand the improvement in SNR consider the results for $B = 8$. Fig. 4 (a) shows the SNR follows the same curve as higher bit-depths until a value of $M = 50$ at which point the curve deviates due to the onset of numerical instability. The point of deviation is increased to $M = 90$ in Fig. 8 (a). Beyond this value of M the SNR reduces and then plateaus.

Fig. 8 (b) shows the number of points used in the RCLCI reconstruction. Generally, it is observed that at small values of M a small number of interpolated points are required to

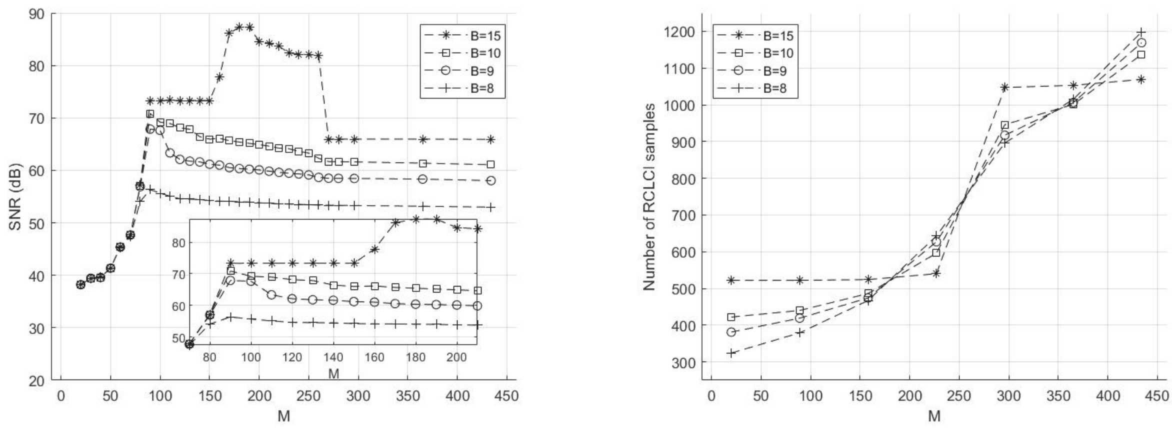

(a) (b)

Fig. 8 (a) SNR and (b) number of RCLCI samples Vs M using RCLCI sampling method on a windowed time speech frame for $C = 0.3$ and 8, 9, 10, 15 bit-depth

ensure the MGC is satisfied. The addition of these points enhances stability and enables reconstruction using a higher value of M, thus interpolation leads to an improvement of the SNR. However, adding more points by increasing M further introduces additional error and the SNR starts to reduce. At sufficiently large M the majority of points are interpolated and hence the SNR becomes dominated by this single source of error and the SNR plateaus. Similar behaviour is observed at all bit-depths although interpolation was not observed to enhance SNR for bit-depths of 10 and 15.

The value of M that optimises the SNR is approximately observed to coincide when $T_{max} = T_{min}$. This condition can be used to calculate the optimal value as $M = \frac{T_0}{2CT_N}$. However, for lower bit-depths SNRs close to the optimal SNR can be achieved for a wide choice of M due to the slow deterioration of the SNR with increasing M.

The behaviour for $B = 15$ in Fig. 8 (b) is seen to be different from that of lower bit-depths and can be understood as follows. As B increases the samples become more uniformly distributed with a sampling interval that approaches T_{min}. For this reason when $M < 200$ we have $T_{max} > T_{min}$ and hence almost all samples satisfy the MGC and no interpolated samples are required. However, for larger values of M, $T_{max} < T_{min}$, nearly all the intervals are interpolated. This is the reason we have a sudden jump in the number of RCLCI samples from $M = 227$ to $M = 296$. For this reason interpolation has no benefit values for $M < 200$ and introduces significant additional error for $M > 300$. The RCLCI algorithm, therefore, appears to bring significant benefit for low bit-depth but is less effective at larger bit-depths.

It is of some interest to compare the RCLCI method to standard ADC theory. We therefore now consider how the SNR depends on the bit-depth. Fig. 9 compares the SNR achieved by RCLCI and CLC methods for $M = 180$ and compares these results to those obtained using a standard uniform sampling method. The value of M was selected because it results in an SNR that is close to optimal for all bit-depths.

Note that the curve for CLC sampling cannot be obtained for bit-depth less than 6 because the condition $J_M \geq 2M + 1$ is not satisfied i.e. there are insufficient data points for the LSP.

First, we note that RCLCI sampling significantly improves the signal SNR compared to CLC for bit-depths less than 12. For bit-depths less than 12 numerical instability becomes a problem for the CLC case and the SNR is consequently compromised. The RCLCI and CLC methods give comparable results at higher bit-depths when the MGC is satisfied but as previously discussed it requires significantly more samples. However, most notable is the linear dependence of the SNR and B. This is reminiscent of the dependence due to quantisation noise observed in standard ADCs and is described by (9). For comparison (9) is shown by the dotted line in Fig. 9 (results labelled theory). Clearly this equation is in reasonable agreement with the RCLCI obtained SNR. We therefore conclude that interpolation introduces a form of quantisation noise. This is perhaps not surprising because the signal, unknown at the point of interpolation, is likely to take on a value between the thresholds of the two samples being interpolated. Due to the RCLC algorithm these thresholds need not to be adjacent but for lower bit-depths are likely to be so. Consequently, an error of the order of the separation of the thresholds is likely as one obtains in standard quantisation. The exact nature of this error is complicated because it depends on the statistics of the signal as well as the positioning of the thresholds.

For comparison the SNR for uniform sampling and reconstructed using the same ACT algorithm is also presented (crosses). Uniform sampling was undertaken to satisfy Nyquist criteria and hence $M = 80$ had to be used to ensure the condition $J_M \geq 2M + 1$ was satisfied. The levels of the uniform samples were also quantised using a standard uniform quantisation.

It is observed that the RCLCI sampling technique delivers a higher SNR in comparison with the uniform sampling method.

For example, the RCLCI technique gives a 7dB improvement compared to uniform for $B = 10$. This result is in keeping with results previously published that also demonstrate that LC techniques can outperform those based on standard sampling methods [29].

Finally, we show why the RCLCI method improves numerical stability. Fig. 10 shows the condition number of the Toeplitz matrix as a function of bit-depth. The RCLCI method ensures that no samples violate the MGC and hence numerical stability is guaranteed. This is shown by the fact the condition number for RCLCI data is approximately one, its minimum theoretical value. In contrast, the uniform sample data lead to an increased condition number because it is sampled using Nyquist criteria, oversampling will in principle reduce it further. And the CLC data have a very high condition number at low bit-depth and is the reason for the numerical instability. Increasing the bit-depth significantly reduces the condition number by eliminating those samples that violate the MGC. As previously described, for bit-depths greater than 12 CLC sampling gives good results albeit with significantly increased samples compared to the RCLC and RCLCI methods.

VIII. Conclusion

New sampling methods in conjunction with ACT reconstruction algorithm are observed to facilitate high fidelity signal reconstruction for speech signals. The results indicate that there is a relationship between the distribution of the data points and the reconstruction accuracy; SNR does not depend on the data points that are closely separated. Therefore, the RCLC sampling technique is proposed which is extremely effective at reducing the number of samples, particularly at high bit-depth where the number of samples increases sublinearly with bit-depth. RCLC achieves reasonable SNRs at sub Nyquist sampling rates. The results also demonstrate that SNR does not depend directly on bit-depth, only on the order of the polynomial M and the maximum gap between samples; the number of violations of MGC does impact adversely on the accuracy of the signal reconstruction. Hence, interpolation between samples is proposed to satisfy MGC; this technique provides numerical stability and makes the Toeplitz matrix well-conditioned. However, RCLCI enhances the SNR at low bit-depths and becomes less effective with increasing bit-depth. The proposed methods could have a potential advantage for reducing data storage/transmission requirements as well as reducing the power of down-stream processing and computational complexity. The criteria for reducing sample density and interpolation would be relatively straightforward to implement in hardware and hence these techniques could lead to practical methodologies.

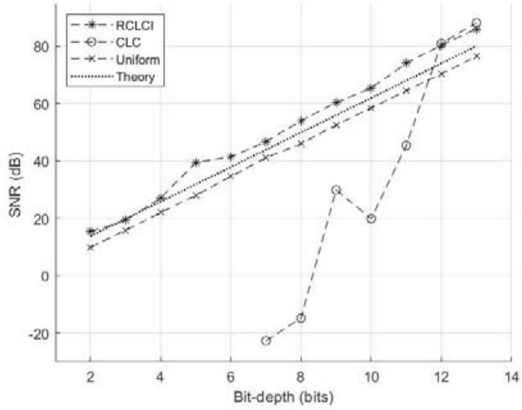

Fig. 9 SNR Vs bit-depth for $C = 0.3$ using RCLCI and CLC methods for $M = 180$ and uniform sampling method for $M = 80$ on a windowed time speech frame

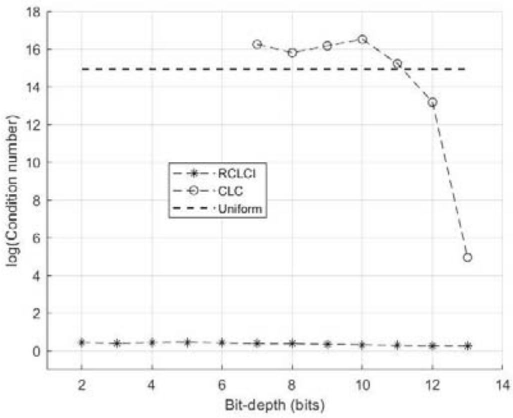

Fig. 10 Condition number Vs bit-depth for $C = 0.3$ using RCLCI and CLC methods for $M = 180$ and uniform sampling method for $M = 80$ on a windowed time speech frame

References

[1] E. Allier, G. Sicard, L. Fesquet and M. Renaudin, "Asynchronous level crossing analog to digital converters," *Meas. J. Int. Meas. Confed.*, vol. 37, pp. 296–309, 2005.

[2] D. Kinniment, A. Yakovlev and B. Gao, "Synchronous and asynchronous A-D conversion," *IEEE Trans. Very Large Scale Integr. Syst.*, vol. 8, pp. 217-220, 2000.

[3] Y. Tsividis, "Event-driven data acquisition and digital signal processing-A tutorial," *IEEE Trans. Circuits Syst. II Express Briefs*, vol. 57, pp. 577-581, 2010.

[4] N. Sayiner, H. V. Sorensen and T. R. Viswanathan, "A level-crossing sampling scheme for A/D conversion," *IEEE Transaction on Circuits and Systems-11: Analog and Digital Signal Processing*, vol. 43, pp. 335-339, 1996.

[5] B. Schell and Y. Tsividis, "A continuous-time ADC/DSP/DAC system with no clock and with activity-dependent power dissipation," *Jssc.*, vol. 43, pp. 2472–2481, 2008.

[6] R. W. Stewart, E. Pine and D. Sweeney, "A digital signal processing audiometric workstation," *IEE.*, 1993.

[7] C. Wijenayake, J. Scutts and A. Ignjatović, "Signal recovery algorithm for 2-level amplitude sampling using chromatic signal approximations," *Signal Processing*, vol. 153, pp. 143–152, 2018.

[8] K. Kozmin, J. Johansson and J. Delsing, "Level-crossing ADC performance evaluation toward ultrasound application," *IEEE Trans. Circuits Syst. I Regul. Pap.*, vol. 56, pp. 1708–1719, 2009.

[9] T. Wang, D. Wang, P. J. Hurst, B. C. Levy and S. H. Lewis, "A level-crossing analog-to-digital converter with triangular dither," *IEEE Trans. Circuits Syst. I Regul. Pap.*, vol. 56, pp. 2089–2099, 2009.

[10] M. Ben-Romdhane, A. Maalej, M. Tlili, C. Rebai, F. Rivet and D. Dallet, "Event-driven ECG sensor in healthcare devices for data transfer optimization," *Arabian Journal for Science and Engineering*, vol. 45, pp. 6361–6387, 2020.

[11] K. Grochenig, "Irregular sampling, Toeplitz matrices, and the approximation of entire functions of exponential type," *Math. Comput.*, vol. 68, pp. 749-765, 2002.

[12] K. Grochenig, "Reconstruction algorithm in irregular sampling," *Math. Comput.*, vol. 59, pp. 181-194, 1992.

[13] J. L. Yen, “On nonuniform sampling of bandlimited signals,” *IRE Trans. Circuit Theory*, vol. 3, pp. 251–257, 1956.

[14] F. J. Beutler, “Error-free recovery of signals from irregularly spaced samples,” *SIAM.*, vol. 8, pp. 328–335, 1966.

[15] C. Vezyrtzis and Y. Tsividis, “Processing of signals using level-crossing sampling,” *Proc. - IEEE Int. Symp. Circuits Syst.*, vol. 37, pp. 2293–2296, 2009.

[16] F. A. Marvasti, *Nonuniform Sampling: Theory and Practice*, Springer, 2001.

[17] E. I. Plotkin, M. N. S. Swamy and Y. Yoganandam, “A novel iterative method for the reconstruction of signal from nonuniformly spaced samples,” *Signal Processing*, vol. 37, pp. 203–213, 1994.

[18] H. Lai, P. Mart and A. V. Oppenheim, “An iterative reconstruction algorithm for amplitude sampling,” *ICASSP.*, pp. 4576–4580, 2017.

[19] R. Kumaresan and N. Panchal, “Encoding bandpass signals using zero/level crossings: A model-based approach,” *IEEE Transactions Audio, Speech Lang. Process.*, vol. 18, pp. 17–33, 2010.

[20] N. K. Sharma and T. V. Sreenivas, “Event-triggered sampling and reconstruction of sparse real-valued trigonometric polynomials,” *Int. Conf. Signal Process. Commun.*, 2014.

[21] U. Grunde, “Non-stationary signal reconstruction from level-crossing samples using akima spline,” *Elektronika Ir Elektrotechnika*, vol. 117, pp. 9–12, 2012.

[22] T. I. Laakso, A. Tarczynski, N. P. Murphy and V. Välimäki, “Polynomial filtering approach to reconstruction and noise reduction of nonuniformly sampled signals,” *Signal Processing*, vol. 80, pp. 567–575, 2000.

[23] J. Y. Rheem, B. H. Kim and S. G. Ann, “A nonuniform sampling method of speech signal and its application to speech coding,” *Signal Processing*, vol. 41, pp. 43-48, 1995.

[24] A. Antony, S. R. Paulson and D. J. Moni, “Asynchronous level crossing ADC design for wearable devices: A review,” *Int. J. Appl. Eng. Res.*, vol. 13, pp. 1858–1865, 2018.

[25] H. G. Feichtinger, K. Grochenig and T. Strohmer, “Efficent numerical methods in non-uniform sampling theory,” *Numer. Math.*, vol. 69, pp. 423-440, 1995.

[26] E. Allier, G. Sicard, L. Fesquet and M. Renaudin, “A new class of asynchronous A/D converters based on time quantization,” *Ninth Int. Symp. Asynchronous Circuits Syst. Proceedings*, pp. 196–205, 2003.

[27] D. Rzepka, M. Miśkowicz, D. Koscielnik and N. T. Thao, “Reconstruction of signals from level-crossing samples using implicit information,” *IEEE Access*, vol. 6, pp. 35001–35011, 2018.

[28] Y. Hou, J. Qu, Z. Tian, M. Atef, K. Yousef, Y. Lian and G. Wang, “A 61-nW level-Crossing ADC with adaptive sampling for biomedical applications,” *IEEE Trans. Circuits Syst. II Express Briefs*, vol. 66, pp. 56–60, 2019.

[29] T. Wu and M. S. Chen, “A subranging-based nonuniform sampling ADC with sampling event filtering,” *IEEE Solid-State Circuits Lett.*, vol. 1, pp. 78–81, 2018.

[30] H. Teimoori, N. Ravanshad and H. Rezaee-Dehsorkh, “Ultra-low-power fully-synchronous level-crossing analog-to-digital converter for bioemdical signal acquisition,” *Int. Conf. Microelectron*, vol. 9, pp. 7–10, 2017.

[31] M. Trakimas and S. Sonkusale, “A 0.8 v asynchronous ADC for energy constrained sensing applications,” *Proc. Cust. Integr. Circuits Conf.*, pp. 173–176, 2008.

[32] T. Strohmer, “Numerical analysis of the non-uniform sampling problem,” *J. Comput. Appl. Math.*, vol. 122, pp. 297-316, 2000.

[33] M. B. Mashhadi, N. Salarieh, E. S. Farahani and F. Marvasti, “Level crossing speech sampling and its sparsity promoting reconstruction using an iterative method with adaptive thresholding,” *IET Signal Process.*, vol. 11, pp. 721–726, 2017.

[34] J. S. Garofolo, L. F. Lamel, W. M. Fisher, J. G. Fiscus, D. S. Pallett, N. L. Dahlgren and V. Zue, “TIMIT acoustic-phonetic continuous speech corpus,” 1993. URL: https://catalog.ldc.upenn.edu/LDC93S1.

[35] J. A. Fernandez and B. V. K. V. Kumar, “Multidimensional overlap-add and overlap-save for correlation and convolution,” *ICIP.*, pp. 509–513, 2013.

[36] M. W. Hauser, “Principles of oversampling A/D conversion,” *J. Audio Eng. Soc.*, vol. 39, pp. 3-26, 1991.

[37] F. James, “On the Runge example,” *Taylor Fr., Ltd . behalf Math. Assoc. Am.*, vol. 94, pp. 329–341, 1987.